Dissipative superfluid hydrodynamics for the unitary Fermi gas

Jiaxun Hou and Thomas Schäfer
Department of Physics, North Carolina State University, Raleigh, North Carolina 27695, USA

(Received 24 May 2021; accepted 26 July 2021; published 13 August 2021)

In this work we establish constraints on the temperature dependence of the shear viscosity η in the superfluid phase of a dilute Fermi gas in the unitary limit. Our results are based on analyzing experiments that measure the aspect ratio of a deformed cloud after release from an optical trap. We discuss how to apply the two-fluid formalism to the unitary gas and provide a suitable parametrization of the equation of state. We show that in expansion experiments the difference between the normal and superfluid velocities remains small and can be treated as a perturbation. We find that expansion experiments favor a shear viscosity that decreases significantly in the superfluid regime. Using an exponential parametrization, we find $\eta(T_c/2T_F) \lesssim 0.37[\eta(T_c/T_F)]$, where T_c is the critical temperature and T_F is the local Fermi temperature of the gas.

DOI: 10.1103/PhysRevA.104.023313

I. INTRODUCTION

The dilute Fermi gas at unitarity has emerged as an important example of a strongly correlated quantum fluid [1,2]. Measurements of equilibrium and nonequilibrium properties provide important benchmarks for a variety of physical systems, ranging from dilute neutron matter in neutron stars to the quark gluon plasma probed in relativistic heavy-ion collisions. The unitary Fermi gas is a system of nonrelativistic spin-$\frac{1}{2}$ particles interacting via an interaction of zero range tuned to infinite scattering length. This means that the system is strongly interacting, but the only scales in the problem are those that can be defined in the noninteracting gas, for example, the Fermi momentum $k_F = (3\pi^2 n)^{1/3}$, where n is the density of the gas. From the Fermi momentum we can construct the Fermi energy $E_F = k_F^2/2m$ and the Fermi temperature $k_B T_F = E_F$, where k_B is the Boltzmann constant. As an example, consider the superfluid transition in a unitary Fermi gas. Based on dimensional analysis, the critical temperature must be proportional to the local Fermi temperature, $T_c \sim T_F$. Indeed, experiments find $T_c = 0.167(3)T_F$ [3].

A remarkable property of the unitary Fermi gas is nearly perfect hydrodynamic flow [4–8], originally discovered in [9]. In this experiment, the authors observed nearly ideal flow in a dilute unitary Fermi gas after release from a deformed trap. The deformation of the trap implies that pressure gradients in the short (transverse) direction of the trap lead to preferential acceleration in this direction. As a consequence, the aspect ratio of the cloud changes from being elongated in the longitudinal direction to being elongated in the transverse direction. Viscosity counteracts this behavior, and detailed studies of the time evolution can be used to extract the shear viscosity as a function of T/T_F.

Shear viscosity is a dimensionful quantity and it is natural to consider the dimensionless ratio η/n or η/s, where s is the entropy density. We have also set $\hbar = k_B = 1$, where $\hbar$ is Planck's constant and k_B is Boltzmann's constant. Previous analysis finds that for $T > T_F$ the shear viscosity of the gas can be understood in terms of kinetic theory and that in this regime $\eta/n > 1$ [10]. Near the critical temperature the shear viscosity enters the quantum regime $\eta/n < 1$ and the viscosity is only weakly temperature dependent. At T_c, we find $\eta/n \simeq 0.4$ [11], in agreement with calculations based on the Kubo relation and resummed perturbation theory [12] (see also [13–15]).

Our main goal in the present work is to constrain the behavior of η/n below the superfluid phase transition using existing expansion experiments, in particular the results of Joseph *et al.* [16]. Several, qualitatively different, predictions and results regarding the behavior of η/n below T_c can be found in the literature. In Ref. [17] we argued that for $T \ll T_c$ kinetic theory in terms of phonon quasiparticles is reliable and that it predicts that η/n grows rapidly as $T/T_F \to 0$. On the other hand, Ref. [18] proposed a different quasiparticle model, which predicts $\eta/n \to 0$ as $T \to 0$. This behavior is seen in the quantum Monte Carlo calculation of [19] and in the simplified experimental analysis in [16]. A recent experimental study of sound attenuation in a unitary Fermi gas found that sound diffusivity is approximately constant below T_c [20]. Different behaviors are also seen in the two isotopes of helium. In ^{4}He the viscosity is dominated by rotons and phonons. It is approximately constant near T_c and grows very steeply as $T \to 0$ [4]. In ^{3}He, on the other hand, the viscosity shows a steep drop below T_c [18,21].

The basic tool for analyzing the expansion experiment below T_c is superfluid (two-fluid) hydrodynamics. When solving the two-fluid equations in an expanding system, careful attention has to be paid to the frame dependence of the equations of motion. We review this issue in Secs. II and III. Section IV discusses simplifications that appear if the fluid is scale invariant, as is the case for the unitary Fermi gas. Sections II–IV can be skipped if the reader is primarily interested in the analysis of the experiments of Joseph *et al.* [16]. Simple solutions of the two-fluid equations are discussed in Sec. V. We discuss an

approach based on treating the difference between the superfluid and normal velocities as a small parameter and present an analysis of the experimental data using this method in Sec. VI. We summarize in Sec. VII. Details regarding the equation of state and the initial conditions for two-fluid hydrodynamics are discussed in several Appendixes.

II. SUPERFLUID HYDRODYNAMICS

Fluid dynamics is based on conservation laws, combined with approximate local thermodynamic equilibrium. Thermodynamic relations are encoded in an equation of state, which can be measured in a fluid at rest in the laboratory frame. In this section we review how this information is used in the fluid dynamics description of an expanding fluid. For simplicity, consider first a normal fluid, for example, the unitary Fermi gas above T_c. There are five hydrodynamic variables, the mass density ρ, the energy density $\mathcal{E}$ (or, alternatively, the entropy density s), and the mass current $\vec{\jmath}$. Note that the mass current is equal to the density of momentum, so the total momentum of the fluid is the integral of $\vec{\jmath}$ over the volume occupied by the fluid.

For a fluid element centered at position $\vec{x}$ with mass current $\vec{\jmath}\,(\vec{x})$ there is a Galilean boost with boost velocity $\vec{v} = \vec{\jmath}/\rho$ that transforms the conserved charges into the local rest frame of the fluid, defined by $\vec{\jmath}\,(\vec{x}) = 0$. In this frame the energy density of the fluid is $\mathcal{E}_0 = \mathcal{E} - \vec{\jmath}^{\,2}/2\rho$ (see Appendix A). The energy density in the rest frame satisfies the standard thermodynamic identity

$$d\mathcal{E}_0 = \mu_0 dn + T ds, \tag{1}$$

where μ_0 is the chemical potential in the fluid rest frame and $n = \rho/m$ is the particle number density. The energy in the laboratory frame satisfies

$$d\mathcal{E} = \left(\mu_0 - \tfrac{1}{2}m\vec{v}^{\,2}\right)dn + T ds + \vec{v}\cdot d\vec{\jmath}. \tag{2}$$

The pressure is given by the Legendre transform of Eq. (2) with respect to n, s, and $\vec{\jmath}$. We obtain $P = \mu_0 n + sT - \mathcal{E}_0$ and the pressure satisfies the Gibbs-Duhem relation $dP = nd\mu_0 + sdT$.

In a superfluid there are three additional hydrodynamic variables, the components of the superfluid velocity $\vec{v}_s$. As a result, there no longer is a unique local frame in which the fluid is at rest. In this section we will follow Landau and Lifshitz [22] and consider thermodynamics in the rest frame of the superfluid. The final result is of course independent of the choice of frame, and we describe thermodynamic relations in the rest frame of the normal fluid in Appendix B. The mass current in the frame of the superfluid is $\vec{\jmath}_0 = \vec{\jmath} - \rho\vec{v}_s$. Using Galilean invariance, we can determine the energy density in the superfluid rest frame

$$\mathcal{E}_s = \mathcal{E} - \vec{\jmath}_0\cdot\vec{v}_s - \tfrac{1}{2}\rho v_s^2. \tag{3}$$

We now view the energy density in the superfluid frame as a function of $\vec{\jmath}_0$,

$$d\mathcal{E}_s = \mu_s dn + T ds + \vec{w}\cdot d\vec{\jmath}_0, \tag{4}$$

where we have defined μ_s, the chemical potential in the superfluid frame, and the velocity $\vec{w}$. For the energy in the laboratory frame Eq. (4) implies

$$d\mathcal{E} = \mu_{J_0} dn + T ds + \vec{v}_n\cdot d\vec{\jmath}_0 + \vec{\jmath}\cdot d\vec{v}_s, \tag{5}$$

where

$$\mu_{J_0} = \mu_s + \tfrac{1}{2}mv_s^2 \tag{6}$$

and we have defined $\vec{v}_n = \vec{w} + \vec{v}_s$, the velocity of the normal fluid. We note that $\vec{w} = \vec{v}_n - \vec{v}_s$ is Galilei invariant. We can perform a Legendre transformation with respect to n, s, and J_0. We obtain the pressure

$$P = -\mathcal{E}_s + \mu_s n + Ts + \vec{\jmath}_0\cdot\vec{w} \tag{7}$$

and the Gibbs-Duhem relation

$$dP = nd\mu_s + sdT + \vec{\jmath}_0\cdot d\vec{w}. \tag{8}$$

Based on Galilean invariance, we can write $\vec{\jmath}_0 = \rho_n\vec{w}$, which defines the normal fluid density ρ_n, as well as the superfluid density $\rho_s = \rho - \rho_n$. This definition leads to the standard two-fluid relation $\vec{\jmath} = \rho_n\vec{v}_n + \rho_s\vec{v}_s$. We note that

$$\rho_n = 2\left.\frac{\partial P}{\partial w^2}\right|_{\mu_s,T}, \tag{9}$$

and $\rho_n \geqslant 0$ implies that at fixed μ_s the pressure increases with $|\vec{w}|$. Finally, we note that

$$P + \mathcal{E} = \mu_s n + Ts + \rho_n\vec{w}\cdot\vec{v}_n + \tfrac{1}{2}\rho v_s^2, \tag{10}$$

which will be useful in the following section.

III. CONSERVATION LAWS

As in ordinary fluid dynamics there are conservation laws for the mass density, the momentum density, and the energy density of the fluid. Mass conservation is

$$\partial_t\rho + \vec{\nabla}\cdot\vec{\jmath} = 0, \tag{11}$$

where $\rho = \rho_n + \rho_s$. The particle density is decomposed analogously, $n = n_n + n_s$. The mass equation does not receive any dissipative corrections. Momentum conservation is

$$\partial_t J_i + \vec{\nabla}_j\Pi_{ij} = 0, \tag{12}$$

where the stress tensor Π_{ij} can be split into an ideal and a dissipative part $\Pi_{ij} = \Pi_{ij}^{(0)} + \delta\Pi_{ij}$. The ideal part is

$$\Pi_{ij}^{(0)} = P\delta_{ij} + \rho_n(v_n)_i(v_n)_j + \rho_s(v_s)_i(v_s)_j. \tag{13}$$

Note that the stress tensor in the superfluid rest frame is $\Pi_{ij}^{(0,s)} = P\delta_{ij} + \rho_n w_i w_j$. This expression follows from Galilean invariance and the second law of thermodynamics. The transformation of Π_{ij} under Galilean boosts is given in Eq. (A5). The dissipative terms are given by

$$\delta\Pi_{ij} = -\eta\sigma_{ij} - \zeta_2\delta_{ij}(\vec{\nabla}\cdot\vec{v}_n) - \zeta_1\vec{\nabla}\cdot(\rho_s\vec{w}), \tag{14}$$

where η is the shear viscosity, the shear tensor is defined by

$$\sigma_{ij} = \vec{\nabla}_i(v_n)_j + \vec{\nabla}_j(v_n)_i - \tfrac{2}{3}\delta_{ij}(\vec{\nabla}\cdot\vec{v}_n), \tag{15}$$

and $\zeta_{1,2}$ are bulk viscosities. In a scale-invariant fluid both ζ_1 and ζ_2 vanish. Energy conservation is

$$\partial_t\mathcal{E} + \vec{\nabla}\cdot\vec{Q} = 0, \tag{16}$$

with $\vec{Q} = \vec{Q}^{(0)} + \delta\vec{Q}$. The ideal energy current in the superfluid rest frame is proportional to $\vec{w}$. Using the second law of thermodynamics, one can show that $\vec{Q}^{(0,s)} = (\mathcal{E}_s + P - n_s\mu_s)\vec{w}$ and the energy current in the laboratory frame is

$$\vec{Q}^{(0)} = \left(\frac{\mu_s}{m} + \frac{v_s^2}{2}\right)\vec{\jmath} + sT\vec{v}_n + \rho_n\left(v_n^2 - \vec{v}_n\cdot\vec{v}_s\right)\vec{v}_n. \quad (17)$$

We observe that with the help of Eq. (10) the energy current $\vec{Q}^{(0)}$ can be expressed as

$$\vec{Q}^{(0)} = \vec{v}_n(\mathcal{E}+P) - \rho_s\vec{w}\left(\frac{\mu_s}{m} + \frac{v_s^2}{2}\right). \quad (18)$$

The dissipative correction is

$$\delta Q_i = -\kappa\vec{\nabla}_i T + \delta\Pi_{ij}(v_n)_j - \delta\chi\rho_s w_i, \quad (19)$$

where κ is the thermal conductivity and $\delta\chi$ is given in Eq. (22). Finally, superfluid hydrodynamics requires an equation of motion for the superfluid velocity. We have

$$\partial_t\vec{v}_s + \vec{\nabla}\chi = 0, \quad (20)$$

where $\chi = \chi^{(0)} + \delta\chi$, with

$$\chi^{(0)} = \frac{\mu_s}{m} + \frac{v_s^2}{2}. \quad (21)$$

The dissipative term is

$$\delta\chi = \zeta_4\vec{\nabla}\cdot\vec{v}_n + \zeta_3\vec{\nabla}(\rho_s\vec{w}). \quad (22)$$

In a scale-invariant gas ζ_4 vanishes [23] but ζ_3 is expected to be nonzero.

IV. UNITARY FERMI GAS

In a normal fluid the pressure is a function of two variables $P = P(\mu_0, T)$. In a scale-invariant fluid we can write

$$P(\mu_0, T) = m^{3/2}\mu_0^{5/2}p(T/\mu_0). \quad (23)$$

In general, the function $p(T/\mu)$ has to be determined from experiment. A parametrization of $p(T/\mu)$ for the dilute Fermi gas at unitarity can be found in [11] and in Appendix C. In a superfluid the pressure is a function of three variables $P(\mu_s, T, \vec{w})$. Using scale invariance, we can define a function p_s of two variables,

$$P(\mu_s, T, \vec{w}) = m^{3/2}\mu_s^{5/2}p_s\left(\frac{T}{\mu_s}, \frac{mw^2}{\mu_s}\right), \quad (24)$$

and for small w we can expand

$$\begin{aligned} P(\mu_s, T, \vec{w}) &= P_0(\mu_s, T) + P_1(\mu_s, T)w^2 \\ &= m^{3/2}\mu_s^{5/2}p_{s0}\left(\frac{T}{\mu_s}\right) \\ &\quad + m^{5/2}\mu_s^{3/2}w^2 p_{s1}\left(\frac{T}{\mu_s}\right). \end{aligned} \quad (25)$$

In a similar fashion, we can expand the density $n = n_0 + n_1 w^2$ and the entropy density $s = s_0 + s_1 w^2$. Note that for $\vec{w} = 0$ we have $\mu_s = \mu_0$ so that the function p_{s0} is determined by the pressure of a fluid at rest $p_{s0}(T/\mu) = p(T/\mu)$. The function p_{s1} is related to the normal fluid density

$$\rho_n = 2m^{5/2}\mu_s^{3/2}p_{s1}\left(\frac{T}{\mu_s}\right). \quad (26)$$

In fluid dynamics we have to determine the pressure using the values of the conserved charges. Consider first a normal scale-invariant fluid. Given the energy density, we can determine the energy density in the rest frame, $\mathcal{E}_0 = \mathcal{E} - \jmath^2/2\rho$. Using the Gibbs-Duhem relation, we get

$$\mathcal{E}_0 = \left\{\mu_0\frac{\partial}{\partial\mu_0} + T\frac{\partial}{\partial T} - 1\right\}P(\mu_0, T). \quad (27)$$

Using the universal form of the equation of state in Eq. (23), this implies $P = \frac{2}{3}\mathcal{E}_0$ and

$$P = \frac{2}{3}\left\{\mathcal{E} - \frac{\jmath^2}{2\rho}\right\}. \quad (28)$$

We observe that the pressure can be determined without using the explicit form of the function $p(T/\mu)$. Note that if the fluid is not scale invariant, then we have to tabulate the equation of state in the form $P = P(\mathcal{E}_0, \rho)$ in order to determine the pressure. We also note that transport coefficients are functions of T/μ_0. The determination of T/μ_0 requires explicit knowledge of the function $p(T/\mu)$. A procedure for extracting T/μ_0 was proposed in [11]. Consider the dimensionless ratio

$$x = \frac{2}{(2\pi)^{3/2}}\frac{(mP)^{3/2}}{n^{5/2}}. \quad (29)$$

The quantity x is Galilean invariant and purely a function of the inverse fugacity $\zeta = \exp(-\mu_0/T)$. The function $\zeta(x)$ can be determined from the function $p(T/\mu)$ defined above. Once ζ is determined we can compute the temperature from

$$T = G(x)\frac{P}{n}, \quad (30)$$

where the dimensionless function $G(x)$ is also determined by $p(T/\mu)$ (see Appendix C). Once ζ and T are given, then the chemical potential is determined by $\mu = -T\ln(\zeta)$.

We can now study the analogous problem in the superfluid phase. We first note that, given the local energy density $\mathcal{E}$, we can compute $\mathcal{E}_s$ using Eq. (3). This calculation only requires the hydrodynamic variables ρ, $\vec{\jmath}$, and $\vec{v}_s$. Furthermore, Eqs. (7) and (8) imply that

$$\mathcal{E}_s = \left\{\mu_s\frac{\partial}{\partial\mu_s} + T\frac{\partial}{\partial T} + \vec{w}\frac{\partial}{\partial\vec{w}} - 1\right\}P(\mu_s, T, w). \quad (31)$$

Using the equation of state of the unitary gas at $O(w^2)$, we get

$$P = \tfrac{2}{3}\left\{\mathcal{E}_s - \tfrac{1}{2}\vec{\jmath}_0\cdot\vec{w}\right\}. \quad (32)$$

This result is more difficult to use than Eq. (28) because, whereas $\mathcal{E}$, $\mathcal{E}_s$, and $\jmath_0$ are (primary) hydrodynamic variables, $\vec{w}$ is determined by the equation of state, $\vec{w} = \vec{\jmath}_0/\rho_n$ with $\rho_n = \rho_n(\rho, \mathcal{E}_s, \jmath_0)$. One possible approach is to tabulate the function $\rho_n(\rho, \mathcal{E}_s, \jmath_0)$ for the equation of state given in Eq. (24). Another option is to solve for ρ_n and P perturbatively in w^2/μ_s.

In the perturbative approach we set[1].

$$P(\{w^0\}) = \tfrac{2}{3}\mathcal{E}_s \tag{33}$$

and define

$$x(\{w^0\}) = \frac{2}{(2\pi)^{3/2}}\frac{[mP(\{w^0\})]^{3/2}}{n^{5/2}}. \tag{34}$$

Here $P(\{w^0\})$ denotes the pressure at order w^0, that is, the exact pressure up to corrections of $O(w^2)$. We can compute the inverse fugacity at this order in the expansion, $\zeta \simeq \zeta(x(\{w^0\}))$, and the result determines the normal fluid fraction at $O(w^0)$,

$$\left(\frac{\rho_n}{\rho}\right)_{\{w^0\}} = \left.\frac{2p_{s1}(x)}{\frac{5}{2}p_{s0}(x) - xp'_{s0}(x)}\right|_{x=x(\{w^0\})}. \tag{35}$$

This result can now be used to compute the pressure at $O(w^2)$,

$$P(\{w^2\}) = \frac{2}{3}\left\{\mathcal{E}_s - \left(\frac{J_0^2}{2\rho}\right)\left(\frac{\rho}{\rho_n}\right)_{\{w^0\}}\right\}. \tag{36}$$

If needed, these results can be used to compute μ_s and T at order w^2.

V. SIMPLE SOLUTIONS OF THE TWO-FLUID EQUATIONS

It is interesting to note that there are some simple solutions to the equations of superfluid hydrodynamics that are relevant to trapped atomic gases. We first observe that the solution of the hydrostatic equation carries over directly from the normal fluid case. Consider a fluid confined by an external potential $V_{\rm ext}(x)$. A static solution of the fluid dynamic equations is given by

$$n(\vec{x}) = n(\mu_s(\vec{x}), T), \quad \mu_s(\vec{x}) = \mu_c - V_{\rm ext}(\vec{x}), \tag{37}$$

with $\vec{v}_n = \vec{v}_s = 0$. This follows directly from the Gibbs-Duhem relation $\vec{\nabla}P = n\vec{\nabla}\mu_s$ for $T = \text{const}$ and $\vec{w} = 0$. We are mostly interested in approximately harmonic potentials of the form $V_{\rm ext}(\vec{x}) = m\omega_i^2 x_i^2/2$. A number of authors have considered small oscillations around the hydrostatic case (see, for example, [24,25]). The solutions are analogous to first and second sound modes in an infinite system.

In the normal fluid case there is a simple exact scaling solution to the Euler equation that describes the expansion after a confining harmonic potential is turned off. For this solution the density expands by a scale transformation $n(x_i, t) = n(x_i/b_i(t), t=0)$, where $n(x_i, 0)$ is a solution of the hydrostatic equation. The velocity field is a Hubble flow $v_i(\vec{x}, t) = \alpha_i(t)x_i$ (no sum over i), where $\alpha_i(t) = \dot{b}_i/b_i$. The temperature T is only a function of time, but not of position. The equation of motion for $b_i(t)$ and $T(t)$ is reviewed in [26,27].

We can ask whether this solution generalizes to a solution of superfluid hydrodynamics in which the normal and superfluid components move together, $\vec{v}_n = \vec{v}_s = \vec{v}$, where $\vec{v}$ is the velocity of a normal fluid satisfying the Euler equation with the equation of state $P(\rho, \mathcal{E}) = P(\rho, \mathcal{E}_s, \vec{w}=0)$. This is indeed the case.

First we note that the momentum density is $\vec{j} = \rho_n\vec{v}_n + \rho_s\vec{v}_s = (\rho_n + \rho_s)\vec{v} = \rho\vec{v}$. This implies that if $\vec{j} = \rho\vec{v}$ satisfies the continuity equations, so does the mass current in superfluid hydrodynamics. The same argument applies to the stress tensor. For $\vec{v}_n = \vec{v}_s$ the stress tensor given in Eq. (13) assumes the normal fluid form $\Pi_{ij}^{(0)} = P\delta_{ij} + \rho v_i v_j$. As a consequence, momentum conservation (12) is satisfied. Finally, we can study the energy current. If $\vec{w} = 0$ then Eq. (18) reduces to $\vec{Q}^{(0)} = \vec{v}(\mathcal{E} + P)$, which is the normal fluid form.

In superfluid hydrodynamics there is one additional equation, which is the equation of motion for the superfluid velocity (20). The superfluid is accelerated by gradients of μ_s, not gradients of P, and Eq. (8) implies that

$$\vec{\nabla}\mu_s = \frac{1}{n}(\vec{\nabla}P - s\vec{\nabla}T - \rho_n w_i\vec{\nabla}w_i). \tag{38}$$

We conclude that the equation of motion for $\vec{v}_s$ follows from the Euler equation provided $\vec{w} = 0$ and $\vec{\nabla}T = 0$. As explained above, these conditions are satisfied for the solution of the Euler equation in an expanding cloud.

The correspondence between the solution of one- and two-fluid hydrodynamics does not extend to the dissipative case, except in very special circumstances. For $\vec{v}_n = \vec{v}_s = \vec{v}$ the dissipative contribution to the stress tensor (14) is given by

$$\delta\Pi_{ij} = -\eta\big[\vec{\nabla}_i v_j + \vec{\nabla}_j v_i - \tfrac{2}{3}\delta_{ij}(\vec{\nabla}\cdot\vec{v})\big] - \zeta_2\delta_{ij}(\vec{\nabla}\cdot\vec{v}), \tag{39}$$

which is the same as the one-fluid expression (for $\zeta = \zeta_2$). However, the viscous correction to the energy current, $\delta Q_i = \delta\Pi_{ij}v_j$ [see Eq. (18)], leads to viscous heating and a nonzero temperature gradient unless the functional form of the viscosity $\eta(n, T)$ is specifically chosen. This implies that we no longer have $\vec{\nabla}P = n\vec{\nabla}\mu_s$, and the solution $\vec{v}_n = \vec{v}_s$ is not consistent.

However, given that viscous corrections are small, we can treat $\vec{\nabla}T$ and $\vec{w}$ as perturbations and solve for $\vec{w}$ at leading order. Using Eqs. (11)–(17), we find

$$\left(\frac{\partial}{\partial t} + \vec{v}\cdot\vec{\nabla}\right)\vec{w} = -\frac{s}{\rho_n}\vec{\nabla}T + O(w^2). \tag{40}$$

In the absence of a background flow $\vec{v} = 0$, this equation is well known from the study of small oscillations in a superfluid, where it describes the restoring force in a second sound mode [22]. We observe that the result remains valid in a nontrivial background flow $\vec{v}_n \simeq \vec{v}_s \neq 0$, provided the advection of $\vec{w}$ in the background flow is taken into account.

VI. HYDRODYNAMIC ANALYSIS IN THE SMALL-*W* LIMIT

In this section we discuss an analysis of the data taken in the superfluid regime by Joseph *et al.* [16]. The same data were previously analyzed in the normal fluid regime in [11]. In the experiments the gas is released from a harmonic trap $V_{\rm ext} = \frac{1}{2}m\omega_i^2 x_i^2$ with trap frequencies $(\omega_x, \omega_y, \omega_z) = 2\pi \times (2210, 830, 64.3)$ Hz. After the optical trap is turned off there is a residual magnetic bowl characterized by $\omega_{\rm mag} = 2\pi \times$

[1]Note that $P(\{w^0\})$ is equal to the exact pressure up to errors of order w^2 but is different from the pressure in the limit $w \to 0$, which we denoted by P_0 in Eq. (25)

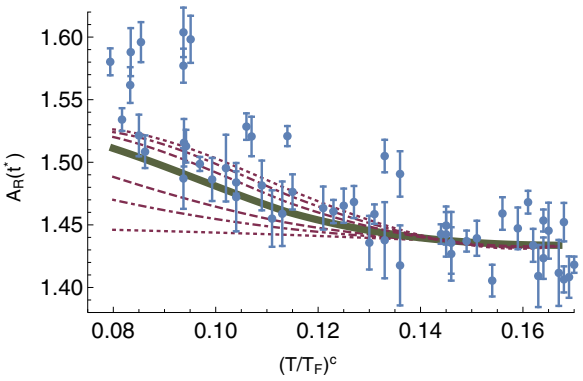

FIG. 1. Aspect ratio A_r as a function of the temperature T/T_F in units of the Fermi temperature at the center of the trap. The data show A_R at $t^* = 1.2 \times 10^{-3}$ s after release from the trap [16]. The lines show the prediction of viscous hydrodynamics for different values of the dimensionless parameter $\alpha = (0, 0.5, 1, 2, 3, 4, 5)$ (from bottom to top) defined in Eq. (43). The thick green line corresponds to $\alpha = 2$.

21.5 Hz. The central temperature of the cloud varies between $T = 0.05T_F$ and $T = 1.10T_F$.

Expansion experiments measure the aspect ratio of the cloud after the gas is released from the harmonic trap. Hydrodynamic flow develops because the pressure gradients in the initial configuration accelerate the gas. If the initial trap is deformed, differences in the pressure gradients in different directions cause the expansion to be fastest in the short direction of the trap. This phenomenon is known as elliptic flow.

Joseph *et al.* [16] measure the ratio $A_R \equiv \sigma_x/\sigma_y$, where σ_x and σ_y are Gaussian fit radii in the x and y direction obtained from two-dimensional absorption images of the cloud. For the trap configuration studied in the experiment, this ratio evolves more quickly than σ_x/σ_z or σ_y/σ_z. Figure 1 shows the dependence of $A_R(t^*)$ at a fixed time $t^* = 1.2$ ms on the initial temperature of the cloud. Note that $A_R(0) \sim 0.37$ and the measured values $A_R(t^*) > 1$ reflect the elliptic flow phenomenon discussed above. The main idea of the experiment is that shear viscosity counteracts the rise in A_R as a function of time and that the dependence of $A_R(t^*)$ on T/T_F constrains the dependence of shear viscosity on temperature and density.

In our previous work we analyzed the data above T_c assuming an expansion of the viscosity in the dimensionless diluteness $n\lambda^3$ of the gas, $\eta(n, T) \simeq \eta_{\rm vir}(n, T)$, with

$$\eta_{\rm vir}(n, T) = \eta_0 (mT)^{3/2} \{1 + \eta_2 (n\lambda^3) + \eta_3 (n\lambda^3)^2 + \cdots\}. \tag{41}$$

Here $\lambda = (2\pi/mT)^{1/2}$ is the thermal de Broglie wavelength. In [11] we obtained

$$\eta_0 = 0.265 \pm 0.02, \quad \eta_2 = 0.060 \pm 0.02. \tag{42}$$

We also found that η_3 is consistent with zero. Note that η_0 can be compared to the kinetic theory result $\eta_0 = 15/(32\sqrt{\pi}) \simeq 0.264$ [28]. Here we will study whether the data constrain the behavior below T_c. We consider the parametrization

$$\eta(n, T < T_c(n)) = \eta_{\rm vir}(n, T) \exp\left(\alpha\left[1 - \frac{T_c(n)}{T}\right]\right), \tag{43}$$

where α is a parameter that governs the low-temperature behavior of the viscosity and $T_c(n) \simeq 0.167(3) T_F(n)$ is the critical temperature for the superfluid transition. This parametrization is sufficiently flexible to accommodate the main possible behaviors of the shear viscosity at low temperature. For $\alpha > 0$ the viscosity tends to zero as $T \to 0$, for $\alpha \simeq 0$ the viscosity is approximately constant, and for $\alpha < 0$ the viscosity diverges as $T \to 0$. We should note that the data mainly constrain the viscosity in the regime $0.5 \lesssim T/T_c \lesssim 1.0$ and that the value of α extracted from our analysis should not be taken as a quantitative prediction for the shear viscosity at very low temperature $T/T_c \lesssim 0.5$.

We analyze the data in the superfluid regime using the results from the preceding section. As a first approximation we will solve the equation using the equation of state in the superfluid regime but assume that the normal and superfluid velocities are equal $\vec{v}_n \simeq \vec{v}_s \equiv \vec{v}$. We will then check this assumption by computing $\vec{w} = \vec{v}_n - \vec{v}_s$ using Eq. (40). We use the equation of state and the initial state described in Appendixes C and D. The equations of fluid dynamics are solved using the anisotropic fluid dynamics method described in [11,29].

The results are shown in Fig. 1. We plot the data for $A_R(t^*)$ as a function of the initial central temperature T/T_F of the cloud. Note that the critical temperature is $T_c/T_F = 0.167(3)$. We also remark that in a trap, the superfluid initially appears in the center of cloud and that near T_c the size of the superfluid core is small (see Appendix D for an illustration of the superfluid and normal density profiles). As a consequence, we observe that in the regime $T/T_c \in [0.8, 1.0]$ the aspect ratio is only very weakly dependent on the viscosity in the superfluid. The data show a noticeable change in slope of A_R as a function of T/T_F at lower temperatures $T \lesssim 0.8T_c$. We find that a good description of the data in this regime can only be achieved if the viscosity at low temperature drops below the extrapolation from the normal phase. It is difficult to fully quantify this statement, because the data contain some outliers and the hydrodynamic prediction for $A_R(t^*)$ is only weakly sensitive to the value of α beyond $\alpha \simeq 5$. Based on Fig. 1, we conclude that the data tend toward $\alpha \gtrsim 2$ (the prediction for $\alpha = 2$ is shown as the thick green line in the figure).

The corresponding behavior of η/n as a function of T/T_F is shown in Fig. 2. We observe that the viscosity exhibits a fairly steep drop below the critical temperature. This behavior is in agreement with the reconstruction performed as part of the original experimental work in [16]. Therein Joseph *et al.* found[2] $\eta(0.8T_c) = (0.32 \pm 0.22)\eta(T_c)$, compared to $\eta(0.8T_c) \simeq 0.53[\eta(T_c)]$ from Fig. 2. The analysis in [16] is based on a number of simplifying assumptions. It assumes, in particular, that there is a critical radial distance in the expansion beyond which the cloud becomes freestreaming. This radius is adjusted to reproduce the theoretically known value of the shear viscosity at large temperature [28]. In our work the transitions to freestreaming happens dynamically, governed by an extended hydrodynamic description that has

[2]To be more precise, if we define $\alpha_n \equiv \eta/n$ as a function of the ratio T/T_F then $\alpha_n[0.8(T/T_F)_c] = 0.32\alpha_n(T/T_F)_c$.

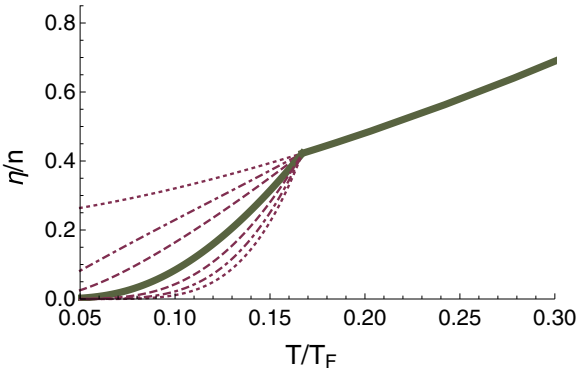

FIG. 2. Viscosity to density ratio η/n as a function of T/T_F, where T_F is the local Fermi temperature. The lines show the fit obtained in this work for different values of the parameter α. The lines are labeled as in Fig. 1. In particular, the thick line corresponds to $\alpha = 2$.

been tested by comparison with exact numerical simulations of the Boltzmann equation [11,30].

Finally, we can go beyond earlier work and test the consistency of the assumption that the normal and superfluid velocities are equal. For this purpose we solve Eq. (40) on the fluid dynamics background of the expanding solution with $\vec{w} = 0$. The viscous heating rate is given by Eqs. (16) and (19),

$$\dot{\mathcal{E}} = \frac{\eta}{2}(\sigma_{ij})^2, \tag{44}$$

where σ_{ij} is the strain tensor defined in Eq. (15). If the viscosity is small then the velocity is approximately linear in distance, and σ_{ij} is spatially constant. This implies that spatial gradients in the rate of energy dissipation are mostly governed by the functional form of the shear viscosity. Note that a possible nonzero ζ_3 does not contribute to energy dissipation in the limit $\vec{w} \to 0$.

The change in temperature is given by $\dot{T} = \dot{\mathcal{E}}/c_V$, where c_V is the specific heat (see Appendix C). Note that c_V drops rapidly as $T/T_F \to 0$, so the spatial structure of the temperature profile is very sensitive to the rate at which η and c_V approach their low-temperature values. The equation of motion for $\vec{w}$ also involves the ratio $s/\rho_n = s/mn_n$. Both the numerator and the denominator vanish in the limit $T \to 0$, but for the unitary Fermi gas the ratio is s/n_n close to unity and only weakly dependent on temperature, as shown in Appendix C. A numerical solution of Eq. (40) is shown in Fig. 3. We observe that spatial variations in dissipative heating do indeed generate a second soundlike perturbation. We note, however, that the amplitude of this perturbation is smaller than the mean fluid velocity by almost two orders of magnitude. This means that the approximation $\vec{w} = 0$ is consistent.

VII. SUMMARY AND OUTLOOK

In this work we have summarized the formalism for applying superfluid hydrodynamics to the dilute Fermi gas at unitarity and constructed a suitable equation of state. We have shown that, unless the viscosity is very large, the equations can be solved perturbatively in the variable $\vec{w} = \vec{v}_n - \vec{v}_s$. We have numerically studied the evolution of a trapped Fermi gas after release from a deformed trap in the regime where the core of the cloud is superfluid. Comparing our simulations to the experimental data obtained in [16] we concluded that the viscosity must drop significantly below T_c. This drop can be parametrized as an exponential decrease proportional to $\exp[-\alpha(T_c/T)]$, where $\alpha \gtrsim 2$.

Our results are in some tension with the data obtained in [20]. Patel *et al.* measured the sound attenuation in a unitary Fermi gas confined in a box trap at approximately constant density and different temperatures, both above and below T_c. They found that the sound diffusivity is approximately constant around T_c and does not exhibit a pronounced decrease. The sound attenuation constant involves several transport coefficients, including the shear viscosity, the thermal conductivity, and, below T_c, the bulk viscosity coefficient ζ_3. These transport coefficients can be disentangled using linear response measurements, as demonstrated in [31], but this analysis has not been performed below T_c. This implies that it is possible that the sound diffusivity remains constant despite the fact that the viscosity is decreasing, but this behavior appears unlikely and is not predicted by any transport theory analysis available in the literature.

It seems more plausible that the difference is explained by differences in the experimental approach. For example, it is possible that the viscosity of the superfluid phase is governed by a fairly dilute gas of quasiparticles, whereas transport in the normal phase is controlled by a system of dense, strongly correlated, excitations. In this case the superfluid core of an

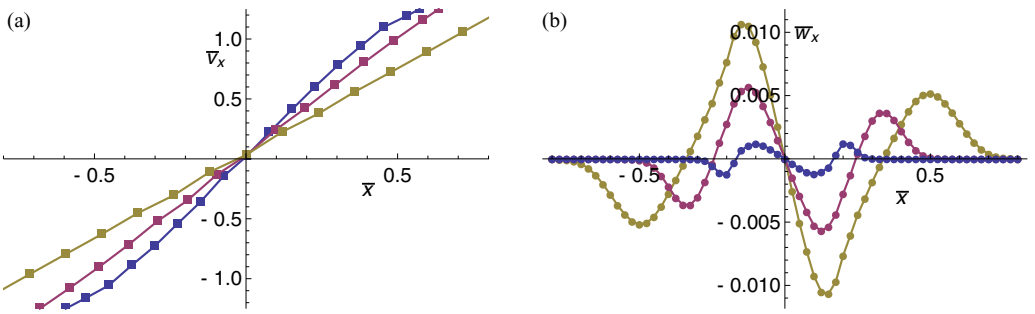

FIG. 3. Perturbative estimate of the superfluid velocity $\vec{w} = \vec{v}_n - \vec{v}_s$. (a) Average velocity in the x direction $v_x \simeq (v_n)_x \simeq (v_s)_x$ from a simulation of trapped gas with central temperature $T/T_F = 0.094$. The position $\bar{x} = x/x_0$ and velocity $\bar{v} = v/v_0$ are given in dimensionless units (see Appendix D). The curves correspond to three different times $t = (0.25, 0.50, 0.75)\bar{\omega}^{-1}$ (blue, red, and olive). (b) Perturbative solution for w_x, as explained in the text. Note that the scale in (b) is two orders of magnitude smaller.

expanding gas cloud might be too small to exhibit dissipative two-fluid dynamics. This option can be addressed by studying linear response in a box trap; an extension of our analysis to these systems is left for future work. The breakdown of superfluid dissipative hydrodynamics is observed in the collective mode experiments [20]. Dissipative fluid dynamics predicts that sound wave damping scales as the wave number squared. This is seen over a wide range of wave numbers above T_c, but only in much narrower window below T_c.

ACKNOWLEDGMENTS

The work of J.H. and T.S. was supported in part by the U.S. Department of Energy Grant No. DE-FG02-03ER41260. We thank J. Thomas and M. Zwierlein for many useful discussions and for providing us with the data published in [3,16].

APPENDIX A: GALILEAN TRANSFORMATIONS

Under a Galilean transformation with boost velocity $\vec{u}$ we have

$$\rho' = \rho, \tag{A1}$$

$$\mathcal{E}' = \mathcal{E} + \vec{\jmath}\cdot\vec{u} + \tfrac{1}{2}\rho u^2, \tag{A2}$$

$$j_i' = j_i + \rho u_i, \tag{A3}$$

$$Q_i' = Q_i + u_j\Pi_{ij} + \tfrac{1}{2}u^2 j_i + \mathcal{E}'u_i, \tag{A4}$$

$$\Pi_{ij}' = \Pi_{ij} + u_i j_j + u_j j_i + u_i u_j \rho, \tag{A5}$$

where ρ is the mass density, $\mathcal{E}$ is the energy density, $\vec{\jmath}$ is the mass current (momentum density), $\vec{Q}$ is the energy current, and Π_{ij} is the stress tensor. The pressure and the entropy density of the fluid are Galilean invariant

$$P' = P, \quad s' = s. \tag{A6}$$

In a superfluid the normal and superfluid densities are separately Galilean invariant. The fluid velocities transforms as

$$\vec{v}_\alpha' = \vec{v}_\alpha + \vec{u}, \tag{A7}$$

where $\alpha = (n, s)$.

APPENDIX B: SUPERFLUID HYDRODYNAMICS IN THE NORMAL FLUID REST FRAME

In Sec. II we studied the thermodynamics of a moving superfluid by constructing the energy density in the superfluid rest frame. This procedure is well defined, even in the limit $T \to T_c$. However, one may be concerned that this method is not the best choice in the limit that the superfluid density is much smaller than the total density of the fluid. In this Appendix we consider an alternative approach based on thermodynamic identities in the rest frame of the normal fluid. Consider the total energy density of a superfluid. Following [32], we write

$$d\mathcal{E} = \mu_J dn + T ds + \vec{v}_n\cdot d\vec{\jmath} + \vec{\jmath}_n\cdot d\vec{v}_s. \tag{B1}$$

which defines $\vec{v}_n$ and $\vec{\jmath}_n$ as variables conjugate to the momentum density $\vec{\jmath}$ and the superfluid velocity $\vec{v}_s$. We use the symbol μ_J to indicate that the chemical potential is defined at fixed $\vec{\jmath}$. Using Galilean invariance, Ref. [32] shows that $\vec{\jmath}_n = \vec{\jmath} - \rho\vec{v}_n$, so that $\vec{\jmath}_n$ is the current in the normal fluid rest frame. We can also write $\vec{\jmath} = \rho_n\vec{v}_n + \rho_s\vec{v}_s$, so that $\vec{\jmath}_n = \rho_s(\vec{v}_s - \vec{v}_n) \equiv -\rho_s\vec{w}$. We obtain the pressure by performing a Legendre transformation

$$P = -\mathcal{E} + \mu_J n + Ts + \vec{v}_n\cdot\vec{\jmath} \tag{B2}$$

so that

$$dP = nd\mu_J + sdT + \vec{\jmath}\cdot d\vec{v}_n - \vec{\jmath}_n\cdot d\vec{v}_s. \tag{B3}$$

Using the explicit form of the currents in terms of the normal and superfluid densities as well as velocities, we find the Gibbs-Duhem relation

$$dP = n\,d\mu_n + s\,dT - \frac{\rho_s}{2}dw^2, \tag{B4}$$

where we have defined the chemical potential in the normal fluid frame

$$\mu_n = \mu_J + \tfrac{1}{2}mv_n^2. \tag{B5}$$

This Gibbs-Duhem relation implies that the superfluid density can be defined as

$$\rho_s = -2\frac{\partial P}{\partial w^2}\bigg|_{\mu_n,T}. \tag{B6}$$

This result should be compared with Eq. (9). We note that the dependence of P on $\vec{w}$ depends crucially on what chemical potential, μ_n or μ_s, is held constant. The energy density in the normal fluid frame can be obtained via a Galilei transformation. We have

$$\mathcal{E}_n = \mathcal{E} - \vec{\jmath}\cdot\vec{v}_n + \tfrac{1}{2}\rho v_n^2, \tag{B7}$$

which implies that the pressure can be written as

$$P = -\mathcal{E}_n + \mu_n n + Ts. \tag{B8}$$

Note that in the normal fluid frame we have the usual (one-fluid) relation $P + \mathcal{E}_n = \mu_n n + sT$.

In a scale-invariant Fermi gas we can write

$$P(\mu_n, T, \vec{w}) = m^{3/2}\mu_n^{5/2}F_n\left(\frac{T}{\mu_n}, \frac{mw^2}{\mu_n}\right). \tag{B9}$$

As before, we can try to simplify the problem by expanding the pressure in $\vec{w}$,

$$P(\mu_n, T, \vec{w}) = m^{3/2}\mu_n^{5/2}p_{n0}\left(\frac{T}{\mu_n}\right) - m^{5/2}\mu_n^{3/2}w^2 p_{n1}\left(\frac{T}{\mu_n}\right). \tag{B10}$$

In the limit $\vec{w} \to 0$ this function must agree with Eq. (25) so that $p_{n0}(s) = p_{s0}(x) = p(x)$. The second function $p_{n1}(x)$ determines the superfluid mass density

$$\rho_s = 2m^{5/2}\mu_0^{3/2}p_{n1}\left(\frac{T}{\mu_n}\right), \tag{B11}$$

which has been measured in [20,33]. Note that ρ_s is positive, so the term proportional to w^2 lowers the pressure at fixed μ_n and T. The energy density in the normal fluid rest frame can be determined using

$$\mathcal{E}_n = \left\{\mu_n\frac{\partial}{\partial\mu_n} + T\frac{\partial}{\partial T} - 1\right\}P, \tag{B12}$$

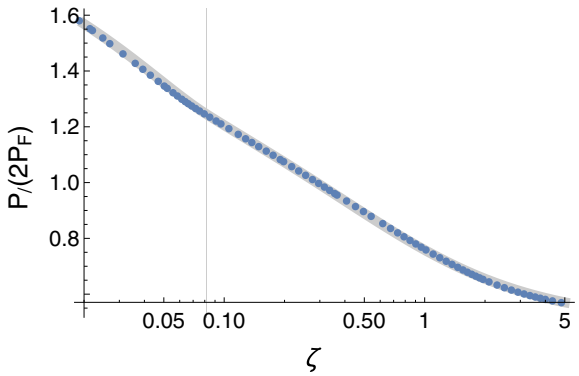

FIG. 4. Pressure $P(\zeta)$ as a function of inverse fugacity $\zeta = \exp(-\mu/T)$ in units of the pressure P_F of a free Fermi gas. The blue circles show the data from [3]. The solid line is our parametrization, which has a discontinuity at $\zeta = \zeta_c = 0.082$.

where $P(\mu_n, T, w)$ is given in Eq. (B10) above. At $O(w^2)$ we find that

$$P = \tfrac{2}{3}\mathcal{E}_n - \tfrac{1}{3}\rho_s w^2. \tag{B13}$$

At this order we also find that

$$P = \tfrac{2}{3}\{\mathcal{E} - \tfrac{1}{2}\rho_n v_n^2 - \tfrac{1}{2}\rho_s v_s^2\}. \tag{B14}$$

Like the results in Sec. II, the expressions (B13) and (B14) are not given in terms of the primary variables $(\mathcal{E}, \rho, \vec{\jmath}, \vec{v}_s)$, and the equation of state is needed to determine ρ_n, ρ_s, and $\vec{v}_n$. This can be accomplished by tabulating the equation of state or by solving for ρ_s iteratively in $\vec{w}$.

APPENDIX C: EQUATION OF STATE

In this Appendix we describe a parametrization of the equation of state of the unitary Fermi gas. We follow the basic strategy described in Appendix B of [11], but we extend the method to the regime below the critical temperature. We begin by considering the pressure of a Fermi gas at rest. We write the pressure as[3]

$$P(T, \mu) = T\lambda^{-3} f(\zeta), \tag{C1}$$

where $\lambda = (2\pi/mT)^{1/2}$ is the thermal de Broglie wavelength and $\zeta = \exp(-\mu/T)$ is the inverse fugacity. In the regime above the critical temperature T_c it is useful to represent the function $f(\zeta)$ in terms of the result for a free Fermi gas

$$f(\zeta) = h(\zeta) p_F(\zeta), \quad p_F(T, \mu) = -Li_{5/2}(-\zeta^{-1}). \tag{C2}$$

The function $h(\zeta)$ was measured in [3] (see Fig. 4). We follow our previous work and parametrize $h(\zeta)$ in the normal fluid regime by a Padé approximant

$$\frac{h(\zeta)}{2} = \frac{\zeta^2 + c_1\zeta + c_2}{\zeta^2 + c_3\zeta + c_4} \quad (\zeta > \zeta_c = 0.082), \tag{C3}$$

with

$$c_1 = 1.321\,09, \quad c_2 = 0.026\,341,$$
$$c_3 = 0.541\,993, \quad c_4 = 0.005\,660. \tag{C4}$$

Here $\zeta_c = 0.082$ is the critical value of the inverse fugacity obtained in [3]. Once the pressure is given, other thermodynamic observables are easily determined. We can write the density and entropy density as

$$n(\mu, T) = \lambda^{-3} g(\zeta), \quad s(\mu, T) = \lambda^{-3} k(\zeta), \tag{C5}$$

where

$$g(\zeta) = -Li_{3/2}(-\zeta^{-1})h(\zeta) + \zeta Li_{5/2}(-\zeta^{-1})h'(\zeta), \tag{C6}$$

$$k(\zeta) = -[\ln(\zeta) Li_{3/2}(-\zeta^{-1}) + \tfrac{5}{2} Li_{5/2}(-\zeta^{-1})]h(\zeta) + \zeta \ln(\zeta) Li_{5/2}(-\zeta^{-1})h'(\zeta). \tag{C7}$$

Other thermodynamic functions can be computed by taking additional derivatives. For example, the specific heat is given by

$$c_V = \frac{T}{V}\frac{\partial S}{\partial T}\bigg|_V = T\left[\frac{\partial s}{\partial T}\bigg|_\mu - \frac{[(\partial n/\partial T)|_\mu]^2}{(\partial n/\partial \mu)|_T}\right]. \tag{C8}$$

The parametrization in Eq. (C3) is quite accurate, even at temperatures below T_c. However, $T = T_c$ is a genuine critical point and the parametrization should exhibit a nonanalyticity at $\zeta = \zeta_c$. Furthermore, Eq. (C3) does not very accurately describe derivatives of the pressure in the regime $\zeta < \zeta_c$. In particular, the entropy density is unphysical for small values of ζ.

In order to address these issues we employ a separate fit of the pressure in the regime $\zeta < \zeta_c$. We have chosen a physically motivated model of the pressure, which is of the form

$$P(\mu, T) = \frac{2^{3/2}\mu^{5/2}m^{3/2}}{15\pi^2\xi^{3/2}} + \frac{\pi^2 T^4}{90}\left(\frac{3m}{2\mu}\right)^{3/2} + A\mu^{5/2}m^{3/2}\sqrt{\frac{T}{\mu}}e^{-\mu B/T}. \tag{C9}$$

Here the first term is the zero-temperature pressure expressed in terms of the Bertsch parameter $\xi = 0.376$. The second term is the contribution of phonons in the superfluid phase (see, for example, Ref. [34]). The third term takes into account thermally excited fermionic quasiparticles, where A and B are treated as fit parameters. The structure of this term is taken from mean-field calculations of the pressure in the BCS limit (see [35]). We fix the values of A and B by requiring the pressure and density to be continuous (but not differentiable) at $\zeta = \zeta_c$. This procedure ensures that the entropy density is continuous as well. We obtain

$$A = 4.6699, \quad B = 2.154\,36. \tag{C10}$$

Note that we have not attempted to reproduce the exact critical behavior of the equation of state, which is expected to be that of the three-dimensional $O(2)$ model. In a harmonic trap, the critical region is only a narrow shell in coordinate space and critical behavior is difficult to observe.

[3]Note that the function $p(x)$ defined in Eq. (23) is given by $p(x) = (2\pi)^{-3/2}x^{5/2}f[\exp(-1/x)]$.

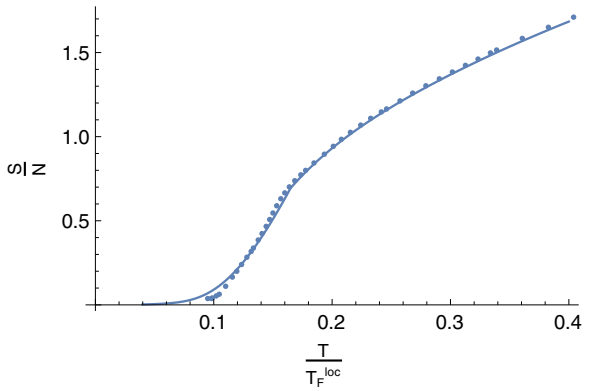

FIG. 5. Entropy per particle S/N as a function of temperature in units of Fermi temperature T/T_F. Here T_F is the local Fermi temperature of the gas, defined by $k_B T_F = k_F^2/2m$, with $k_F^3 = 3\pi^2 n$. The data points are from [3].

In terms of the functions $f(\zeta)$ and $g(\zeta)$ defined in Eqs. (C1) and (C5), the low-temperature model of the equation of state is

$$f_s(\zeta) = \frac{2^{5/2}(2\pi)^{3/2}}{15\pi^2\xi^{3/2}}[-\ln(\zeta)]^{5/2} + \frac{\pi^2(2\pi)^{3/2}}{90}\left(\frac{3}{2}\right)^{3/2} \times [-\ln(\zeta)]^{-3/2} + A(2\pi)^{3/2}[\ln(\zeta)]^2\zeta^B, \quad \text{(C11)}$$

$$g_s(\zeta) = \frac{2^{5/2}(2\pi)^{3/2}}{6\pi^2\xi^{3/2}}[-\ln(\zeta)]^{3/2} - \frac{\pi^2(2\pi)^{3/2}}{90}\left(\frac{3}{2}\right)^{5/2} \times [-\ln(\zeta)]^{-5/2} - A(2\pi)^{3/2} \times [2 + B\ln(\zeta)]\ln(\zeta)\zeta^B, \quad \text{(C12)}$$

where $f_s(\zeta) = f(\zeta < \zeta_c)$ and $g_s(\zeta) = g(\zeta < \zeta_c)$. Equations (C1)–(C3) and (C11) define our equation of state. To illustrate the accuracy of this parametrization, we show in Fig. 4 the pressure as a function of ζ and in Fig. 5 the entropy per particle as a function of T/T_F, both compared to the experimental results of Ku *et al.* [3].

In fluid dynamics we have to reconstruct ζ from the density and pressure of the gas. For this purpose we consider the function

$$F(\zeta) = \frac{2f(\zeta)^{3/2}}{g(\zeta)^{5/2}}, \quad \text{(C13)}$$

where $f(\zeta)$ and $g(\zeta)$ are defined piecewise for ζ larger and smaller than ζ_c. The function $F(\zeta)$ is proportional to the dimensionless ratio $(mP)^{3/2}/n^{5/2}$. We have

$$\zeta = F^{-1}\left(\frac{2}{(2\pi)^{3/2}}\frac{(mP)^{3/2}}{n^{5/2}}\right). \quad \text{(C14)}$$

The function $F(\zeta)$ is defined so that $F(\zeta \gg \zeta_c) \simeq \zeta$, and as a result $F^{-1}(x \gg x_c) \simeq x$. We show $F^{-1}(x)$ for all x in Fig. 6. Note that there is a minimum value of x, given by $x_0 = F(0)$. In practice, we employ parametrization of $F^{-1}(x)$. This function is also defined piecewise for $x > x_c$ (corresponding to $T > T_c$) and $x < x_c$ (the regime $T < T_c$), where $x_c = 0.1285$.

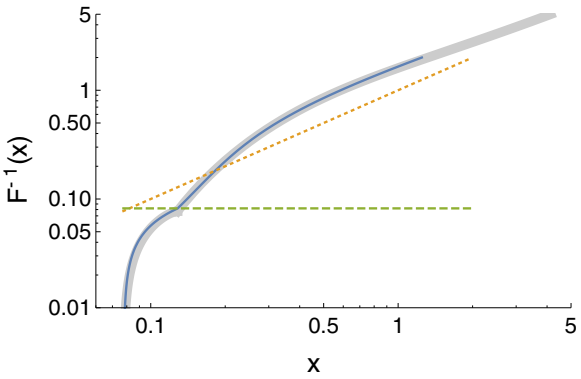

FIG. 6. Plot of the function $\zeta = F^{-1}(x)$ that determines the inverse fugacity in terms of a dimensionless ratio of the pressure and the density, $x \sim (mP)^{3/2}/n^{5/2}$. The blue solid line shows the two-component fit to the pressure and density. The green dashed horizontal line is $\zeta_c = 0.082$ and the orange dotted line is the high-temperature limit $F^{-1}(x) \simeq x$. The gray band is a fit to $F^{-1}(x)$ described in the text.

For $x > x_c$ we again use a Padé approximant

$$F_{\rm fit}^{-1}(x) = x\frac{1 + h_1/x + h_2/x^2}{1 + h_3/x + h_4/x^2} \quad (x > x_c = 0.1285), \quad \text{(C15)}$$

with

$$h_1 = 1.1601, \quad h_2 = -0.0927, \quad h_3 = 0.2119, \quad h_4 = 0.077\,29. \quad \text{(C16)}$$

In the superfluid regime $x < x_c$ we write

$$F_{\rm fit}^{-1}(x) = \zeta_c^{\rm fit}\left\{1 - \left(\frac{x_c - x}{x_c - x_0}\right)^{3/2}\right\}^{2/3}, \quad \text{(C17)}$$

with

$$\zeta_c^{\rm fit} = 0.077\,32, \quad x_c = 0.1285, \quad x_0 = 0.0775. \quad \text{(C18)}$$

The function $F^{-1}(x)$, together with the fit given above, is shown in Fig. 6.

Finally, given the local fugacity, we have to determine the temperature and chemical potential of the fluid. In the high-temperature limit this is straightforward; we can use $T = P/n$. In the general case we can write

$$T = G(x)\frac{P}{n}, \quad \text{(C19)}$$

where $G(x)$ is a correction factor, given by

$$G(x) = \frac{g(\zeta(x))}{f(\zeta(x))} = \frac{g(F^{-1}(x))}{f(F^{-1}(x))}. \quad \text{(C20)}$$

The function $G(x)$ extracted from our parametrization of the pressure and density is shown in Fig. 7. We note that for $x > x_c$ the function $G(x)$ is close to the high-temperature limit $G = 1$. In the low-temperature regime $x < x_c$ the correction factor $G(x)$ drops very steeply, with $G(x_0) = 0$ at $x_0 = 0.0775$. This behavior results in a simple two-component fit, similar to the one for $F^{-1}(x)$. We write

$$G_{\rm fit}(x) = \frac{1 + d_1/x + d_2/x^2}{1 + d_3/x + d_4/x^2} \quad (x > x_c = 0.1285), \quad \text{(C21)}$$

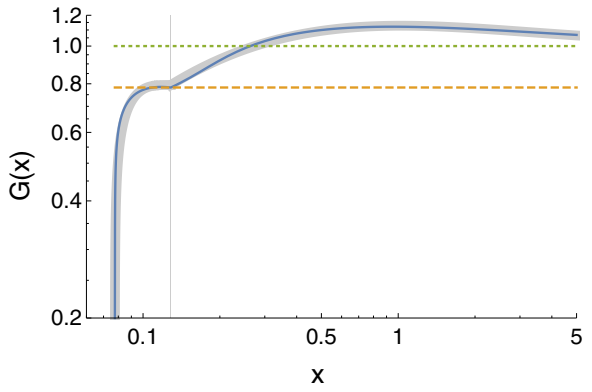

FIG. 7. Temperature correction factor $G(x) = P/nT$ as a function of the dimensionless variable $x \sim (mP)^{3/2}/n^{5/2}$. The blue solid line shows the two-component fit to the pressure and density. The green dotted horizontal line is the high-temperature limit $G = 1$ and the orange dashed line shows the critical value G_c. The gray band is a fit to $G(x)$ described in the text.

with

$$d_1 = 1.8052, \quad d_2 = -0.0022,$$
$$d_3 = 1.3668, \quad d_4 = 0.1179. \tag{C22}$$

In the superfluid regime $x < x_c$ we write

$$G_{\rm fit}(x) = G_c^{\rm fit}\left\{1 - \left(\frac{x_c - x}{x_c - x_0}\right)^4\right\}^{1/4}, \tag{C23}$$

with $G_c^{\rm fit} = 0.7944$.

As explained in the main text, in the superfluid phase there is an additional thermodynamic function, the superfluid mass density $\rho_s(\mu, T)$. The superfluid mass fraction was determined in [33] (see also the recent work in [20]). We show the results of [33] in Fig. 8. A simple quasiparticle model for these results is discussed by Baym and Pethick [36]. Here we

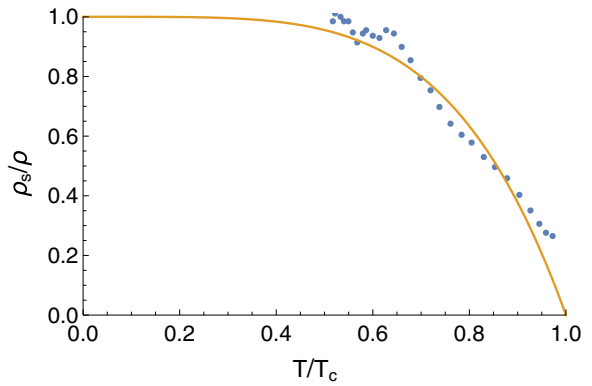

FIG. 8. Superfluid mass fraction ρ_s/ρ as a function of the temperature T in units of the local Fermi temperature T_F. The points show the data from [33] and the line shows the fit discussed in the text. Note that the data points have uncertainties of order 10%, in both T/T_F and ρ_s/ρ, that are not shown here.

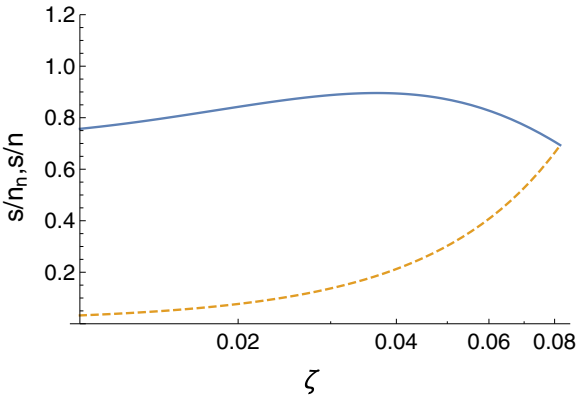

FIG. 9. Entropy density over superfluid density (solid line) and entropy density over total density (dashed line) in the superfluid regime, plotted as a function of the inverse fugacity ζ.

use an even simpler parametrization, given by

$$\frac{\rho_s}{\rho} = 1 - \left(\frac{T}{T_c}\right)^{9/2}, \tag{C24}$$

where T_c is the critical temperature. This parametrization is not directly induced by a physical model, but is numerically close to the theory of Baym and Pethick. Note that the superfluid density of a dilute Bose gas scales as $\rho_s/\rho = 1 - (T/T_c)^{3/2}$. Finally, based on this result, we can compute the ratio of the entropy density over the normal fluid density, which enters the equation for the acceleration of $\vec{w}$ [see Eq. (40)]. The result is shown in Fig. 9.

APPENDIX D: TRAPPED FERMI GAS

A trapped Fermi gas in thermal equilibrium is a solution of the hydrostatic equation. As explained in Sec. V, in both the normal and the superfluid regime the solution is given by

$$n(\vec{x}, t) = n(\mu_s(\vec{x}), T), \quad \mu_s(\vec{x}) = \mu_c - V_{\rm ext}(\vec{x}). \tag{D1}$$

In the experiment we consider trapped clouds with a given number of particles N at a fixed temperature T or total energy E. Given N and T, the central inverse fugacity $\zeta_0 = \zeta(0)$ is fixed by the condition

$$\frac{3}{(2\pi)^3}\left(\frac{T}{T_F^{\rm trap}}\right)\int d^3x\, g\left(\zeta_0 \exp\left(\frac{x^2}{2}\right)\right) \equiv 1, \tag{D2}$$

where $T_F^{\rm trap} = 3N^{1/3}\bar{\omega}$ is the Fermi temperature of the trap. Once ζ_0 is determined the total energy can be computed using the virial theorem. Making use of the virial theorem, we can calculate the energy of the trapped gas

$$\frac{E}{NE_F^{\rm trap}} = \left(\frac{T}{T_F^{\rm trap}}\right)^3 \frac{\int d^3x\, x^2 g\left(\zeta_0 \exp\left(\frac{x^2}{2}\right)\right)}{\int d^3x\, g\left(\zeta_0 \exp\left(\frac{x^2}{2}\right)\right)}. \tag{D3}$$

Figure 10 shows $E/NE_F^{\rm trap}$ as a function of $T/T_F^{\rm trap}$ for a harmonically trapped Fermi gas. The critical temperature and energy, that is, the values of T and E at which superfluidity appears at the center of the trap, are

$$T_c/T_F^{\rm trap} = 0.222, \quad E_c/NE_F^{\rm trap} = 0.695. \tag{D4}$$

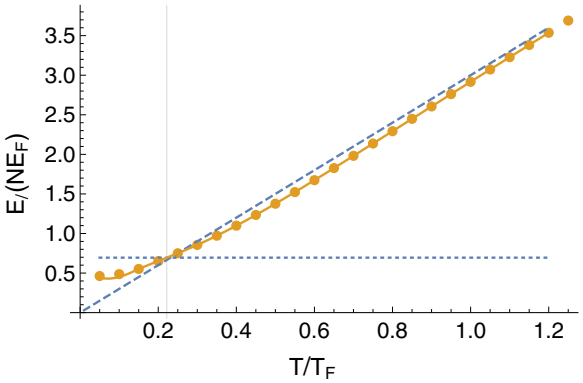

FIG. 10. Energy versus temperature for a harmonically trapped Fermi gas. The energy is given in units of $NE_F^{\rm trap}$, where $E_F^{\rm trap} = 3N^{1/3}\bar{\omega}$. The temperature is given in units of $T_F^{\rm trap} = E_F^{\rm trap}$ (where $k_B = 1$). The points are computed from our parametrization of the equation of state and the dotted line is an interpolating function. The dashed diagonal line corresponds to the high-temperature limit $E = \frac{3}{2}T$. The horizontal and vertical lines indicate the critical values $T_c/T_F^{\rm trap} = 0.222$ and $E_c/E_F^{\rm trap} = 0.695$, respectively.

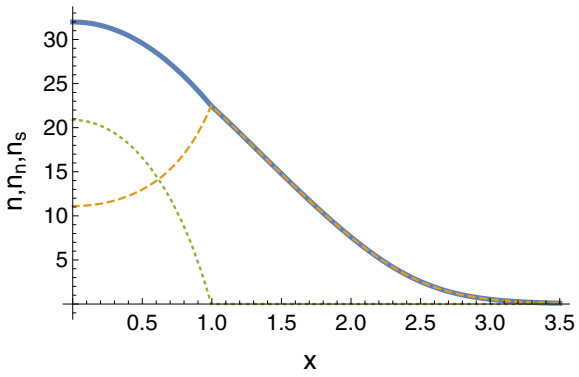

FIG. 11. Density profile of a harmonically trapped Fermi gas below the critical temperature at which superfluidity appears at the center of the trap. We show the total (blue solid line), normal (orange dashed line), and superfluid (green dotted line) densities n, n_n, and n_s, respectively, in units of λ^{-3} as a function of x in units of the length x_0 defined in the text. Here the central inverse fugacity was chosen as $\zeta_0 = 0.05$.

The zero-temperature limit of the energy is $E_0/NE_F^{\rm trap} = (3\sqrt{\xi})/4 = 0.460$.

An example of the density profile of a harmonically trapped Fermi gas in the superfluid regime is shown in Fig. 11. In this example the inverse fugacity at the trap center is $\zeta_0 = 0.05$, corresponding to a central temperature $T/T_F = 0.13$. We note that there is a two-fluid mixture in the core. The superfluid appears at some critical radius x_c, but the total density only shows a very mild nonanalyticity at x_c. In the figure the position x is shown in dimensionless units $\bar{x} = x/x_0$ with

$$x_0 = \left[\frac{2}{3}\frac{(3N)^{1/3}}{m\bar{\omega}}\right]^{1/2}. \tag{D5}$$

Similar dimensionless units can be employed for time $\bar{t} = t/t_0$ with $t_0 = \bar{\omega}^{-1}$ and velocity $\bar{v} = v/v_0$ with $v_0 = t_0/x_0$. In our hydrodynamic simulations we also use dimensionless variables for thermodynamic quantities, such as density $\bar{n} = n/n_0$, pressure $\bar{P} = P/P_0$, temperature $\bar{T} = T/T_0$, and viscosity $\bar{\eta} = \eta/\eta_0$,

$$n_0 = x_0^{-3}, \quad P_0 = m\bar{\omega}^2 x_0^{-1}, \quad T_0 = m\bar{\omega}^2 x_0^2, \quad \eta_0 = m\bar{\omega}x_0^{-1}. \tag{D6}$$

[1] I. Bloch, J. Dalibard, and W. Zwerger, Many-body physics with ultracold gases, Rev. Mod. Phys. **80**, 885 (2008).

[2] S. Giorgini, L. P. Pitaevskii, and S. Stringari, Theory of ultracold atomic Fermi gases, Rev. Mod. Phys. **80**, 1215 (2008).

[3] M. J. H. Ku, A. T. Sommer, L. W. Cheuk, and M. W. Zwierlein, Revealing the superfluid lambda transition in the universal thermodynamics of a unitary Fermi gas, Science **335**, 563 (2012).

[4] T. Schäfer and D. Teaney, Nearly perfect fluidity: From cold atomic gases to hot quark gluon plasmas, Rep. Prog. Phys. **72**, 126001 (2009).

[5] A. Adams, L. D. Carr, T. Schäfer, P. Steinberg, and J. E. Thomas, Strongly correlated quantum fluids: Ultracold quantum gases, quantum chromodynamic plasmas, and holographic duality, New J. Phys. **14**, 115009 (2012).

[6] T. Schäfer, Fluid dynamics and viscosity in strongly correlated fluids, Annu. Rev. Nucl. Part. Sci. **64**, 125 (2014).

[7] T. Schäfer, The shear viscosity to entropy density ratio of trapped fermions in the unitarity limit, Phys. Rev. A **76**, 063618 (2007).

[8] A. Turlapov, J. Kinast, B. Clancy, L. Luo, J. Joseph, and J. E. Thomas, Is a gas of strongly interacting atomic fermions a nearly perfect fluid, J. Low Temp. Phys. **150**, 567 (2008).

[9] K. M. O'Hara, S. L. Hemmer, M. E. Gehm, S. R. Granade, and J. E. Thomas, Observation of a strongly-interacting degenerate Fermi gas of atoms, Science **298**, 2179 (2002).

[10] M. Bluhm and T. Schäfer, Model-Independent Determination of the Shear Viscosity of a Trapped Unitary Fermi Gas: Application to High Temperature Data, Phys. Rev. Lett. **116**, 115301 (2016).

[11] M. Bluhm, J. Hou, and T. Schäfer, Determination of the Density and Temperature Dependence of the Shear Viscosity of a Unitary Fermi Gas Based on Hydrodynamic Flow, Phys. Rev. Lett. **119**, 065302 (2017).

[12] T. Enss, R. Haussmann, and W. Zwerger, Viscosity and scale invariance in the unitary Fermi gas, Ann. Phys. (NY) **326**, 770 (2011).

[13] J. Hofmann, Current response, structure factor and hydrodynamic quantities of a two- and three-dimensional Fermi gas from the operator product expansion, Phys. Rev. A **84**, 043603 (2011).

[14] J. Hofmann, High-temperature expansion of the viscosity in interacting quantum gases, Phys. Rev. A **101**, 013620 (2020).
[15] B. Frank, W. Zwerger, and T. Enss, Quantum critical thermal transport in the unitary Fermi gas, Phys. Rev. Research **2**, 023301 (2020).
[16] J. A. Joseph, E. Elliott, and J. E. Thomas, Shear Viscosity of a Universal Fermi Gas Near the Superfluid Phase Transition, Phys. Rev. Lett. **115**, 020401 (2015).
[17] G. Rupak and T. Schäfer, Shear viscosity of a superfluid Fermi gas in the unitarity limit, Phys. Rev. A **76**, 053607 (2007).
[18] H. Guo, D. Wulin, C.-C. Chien, and K. Levin, Perfect fluids and bad metals: Transport analogies between ultracold Fermi gases and high T_c superconductors, New J. Phys. **13**, 075011 (2011).
[19] G. Wlazlowski, P. Magierski, A. Bulgac, and K. J. Roche, The temperature evolution of the shear viscosity in a unitary Fermi gas, Phys. Rev. A **88**, 013639 (2013).
[20] P. Patel, Z. Yan, B. Mukherjee, R. Fletcher, J. Struck, and M. Zwierlein, Universal sound diffusion in a strongly interacting fermi gas, Science **370**, 1222 (2020).
[21] D. Vollhardt and P. Wölfle, *The Superfluid Phases of Helium 3* (Taylor & Francis, Philadelphia, 1990).
[22] L. D. Landau and E. M. Lifshitz, *Fluid Mechanics*, Course of Theoretical Physics Vol. 6 (Pergamon, Oxford, 1984).
[23] D. T. Son, Vanishing Bulk Viscosities and Conformal Invariance of Unitary Fermi Gas, Phys. Rev. Lett. **98**, 020604 (2007).
[24] E. Zaremba, T. Nikuni, and A. Griffin, Dynamics of trapped Bose gases at finite temperatures, J. Low Temp. Phys. **116**, 277 (1999).
[25] Y.-H. Hou, L. P. Pitaevskii, and S. Stringari, Scaling solutions of the two-fluid hydrodynamic equations in a harmonically trapped gas at unitarity, Phys. Rev. A **87**, 033620 (2013).
[26] T. Schäfer and C. Chafin, in *The BCS-BEC Crossover and the Unitary Fermi Gas*, edited by W. Zwerger, Lecture Notes in Physics Vol. 836 (Springer, Cham, 2012), pp. 375–406.
[27] T. Schäfer, Dissipative fluid dynamics for the dilute Fermi gas at unitarity: Free expansion and rotation, Phys. Rev. A **82**, 063629 (2010).
[28] G. M. Bruun and H. Smith, Viscosity and thermal relaxation for a resonantly interacting Fermi gas, Phys. Rev. A **72**, 043605 (2005).
[29] M. Bluhm and T. Schäfer, Dissipative fluid dynamics for the dilute Fermi gas at unitarity: Anisotropic fluid dynamics, Phys. Rev. A **92**, 043602 (2015).
[30] P. A. Pantel, D. Davesne, and M. Urban, Numerical solution of the Boltzmann equation for trapped Fermi gases with in-medium effects, Phys. Rev. A **91**, 013627 (2015).
[31] L. Baird, X. Wang, S. Roof, and J. E. Thomas, Measuring the Hydrodynamic Linear Response of a Unitary Fermi Gas, Phys. Rev. Lett. **123**, 160402 (2019).
[32] T.-L. Ho and V. B. Shenoy, The hydrodynamic equations of superfluid mixtures in magnetic traps, J. Low. Temp. Phys. **111**, 937 (1998).
[33] L. Sidorenkov, M. Tey, R. Grimm, L. Pitaevski, and S. Stringari, Second sound and the superfluid fraction in a Fermi gas with resonant interactions, Nature (London) **498**, 78 (2013).
[34] M. Braby, J. Chao, and T. Schäfer, Thermal conductivity and sound attenuation in dilute atomic Fermi gases, Phys. Rev. A **82**, 033619 (2010).
[35] A. A. Abrikosov, L. P. Gorkov, and I. E. Dzyaloshinski, in *Methods of Quantum Field Theory in Statistical Physics*, edited by R. A Silverman (Dover, New York, 1963).
[36] G. Baym and C. J. Pethick, Normal mass density of a superfluid Fermi gas at unitarity, Phys. Rev. A **88**, 043631 (2013).